INTERNATIONAL JOURNAL OF MEDICAL SCIENCE AND DENTAL HEALTH
(ISSN: 2454-4191)
www.ijmsdh.org (2026)

Check for updates

Received: 11 Mar 2026
Revised: 10 Apr 2026
Accepted: 22 May 2026
Published: 12 June 2026

Page No - 24-33
DOI - 10.55640/ijmsdh-12-06-03

Article Citation: Albonwas, R. kamel. (2026). Spatial Clustering Analysis of Mortality Tuberculosis in The Iraq, 2018 To 2022. International Journal of Medical Science and Dental Health, 12(06), 24-33. https://doi.org/10.55640/ijmsdh-12-06-03

Copyright: © 2026 The Authors. Published by IJMSDH under the Creative Commons CC BY License

Spatial Clustering Analysis of Mortality Tuberculosis in The Iraq, 2018 To 2022

Rana kamel Albonwas
Department of Basic sciences, Faculty of Dentistry, University of Kufa, Al-Najaf, Iraq

Abstract

Back ground: Iraq's Environmental Statistics and Health Indicators published annual mortality rates for tuberculosis from 2018 to 2022. However, this publication does not assess whether the patterns are merely the result of chance or whether they accurately reflect regional variations in disease risk or treatment methods. To formally test for geographical clustering of disease, we used global spatial autocorrelation to analyze Iraq's annual TB mortality rates from 2018 to 2022. The spatial scan statistic, the Anselin Local Moran's I, and Getis-Ord Gi* were used to determine the spatial variations of TB mortality rates. Geographic clustering was statistically significant across all age and gender groups, according to all tests. The spatial scan statistic indicated that the most likely cluster of high mortality was in parts of Dha qar, Maysan, Basrah, Diwaniyah, Muthanna, Wasit, Babil, Najaf, and Karbala, (LLR= 4.71, $P < 0.05$). Secondary clusters were found in Ninawa, Dahuk, Karbala, Arbil, Tam'mim, Salah ad din, Sulaymaniyah, Diyala, and Anbar (LLR= 0.88, $P > 0.05$). For 25% maximum window size, the statistically significant most likely was found around Diwaniyah, Babil, Wasit, Karbala, Dha qar, and Najaf (LLR= 3.65, $P < 0.05$), with secondary clusters in Ninawa, Dahuk, Karbala, Arbil, Tam'mim, Salah ad din, Sulaymaniyah, Diyala, and Anbar (LLR= 0.88, $P > 0.05$).

Keywords: Iraq, Tuberculosis (TB), Moran's I, Anselin Local Moran's I and Getis-Ord Gi*

1. Introduction

Anyone can get infectious tuberculosis, or TB, which is one of the world's major causes of death and illness. Prior to the COVID-19 pandemic, tuberculosis (TB) was the leading infectious disease-related cause of death. The treatability and preventability of tuberculosis (TB) are higher than those of HIV/AIDS. About 85% of patients with TB disease respond well

to a six-month pharmaceutical therapy [1]. Despite international efforts to manage the disease, many people are still infected with tuberculosis (TB), an infectious disease caused by Mycobacterium tuberculosis. The World Health Organization (WHO) estimates that 10 million individuals worldwide suffered with tuberculosis (TB) in 2018, which resulted in 1.5 million fatalities [2]. However, according to WHO data, up until 2015, only 61% of TB patients have been identified [3].Each nation must identify high-risk locations in order to achieve the ultimate objective of TB elimination by 2050, which is defined as ≤1 case per 1 million people [4]. With Geographic Information Systems (GIS) techniques [5–9], which store data by two components: spatial and non-spatial, it is possible to identify spatial and spatiotemporal patterns of diseases [10–13]. While the latter contains additional information, such as patient data like age, gender, etc., the former is dependent on geography, such as the patient's place of residence. By performing spatio-temporal studies that integrate spatial and non-spatial data and take the time component into account, GIS makes it possible to visualize and track infectious diseases [14]. Data distributions and patterns are found in the context of both space and time using spatiotemporal pattern analysis [15]. Spatial scan statistics' TB study in Pakistan [16] found spatiotemporal clustering with high-risk clusters throughout the nation from 2015 to 2019, especially in the study area's northern and western regions. Another study used empirical Bayesian and Moran statistics to evaluate the temporal and spatial patterns of tuberculosis in 75 municipalities in northeastern Brazil between 2001 and 2016 [7]. observed a rise in the prevalence of tuberculosis in patients younger than 40. According to Masabarakiza et al. [17], who using GIS to analyze the distribution of TB incidence in Burundi from 2009 to 2017, the country's eastern regions showed comparatively low TB incidence rates when compared to other regions. According to a Western Kenyan retrospective study [9], which examined the spatial distribution of 23,374 TB cases from 2012 to 2015, the small-area TB incidence ranged from 638.0 to 121.4 individuals per 100,000. They were able to identify 16 districts with a high incidence of tuberculosis by using geographic clustering analysis based on the Moran and Getis-Ord Gi* statistic [18]. When someone coughs or talks, the majority of the droplets that are discharged from their mouth, nose, and throat spread the respiratory illness TB. Other parts of the body, including the lymph nodes, pleura, belly and urogenital tract [19, 20], skin and joints [21, 22], bones [23, 24], and meninges, can also get infected with tuberculosis. This later form of the disease is called extrapulmonary tuberculosis. The World Health Organization (WHO) defines an LTBI as an ongoing immunological response to Mycobacterium tuberculosis (M. tb) antigens, even in the absence of tuberculosis signs or symptoms. The World Health Organization (WHO) estimates that by 2020, there will be 27 cases of tuberculosis per 100,000 people in Iraq [25]. To the best of our knowledge, the present study would be the first epidemiological exploration on solely geographic TB death clusters in the country of Iraq.

2. Data and methods

The Department of Health and Life Statistics Iraq provided the 18 provinces' statistics on tuberculosis (TB) mortality for the years 2018–2022. The Central Bureau of Statistics Iraq provided population estimates for each of the 18 provinces for each of the years 2018–2022. By connecting and matching the TB mortality data with the shape file vector map that we acquired from the Directorate of Water Resources in Najaf, we were able to generate an extensive geographical analysis database.

Spatial autocorrelation analysis

The global pattern of TB mortality occurrence was examined using the Global Mora's I approach. The degree of resemblance between a particular site and its surrounding units was evaluated using spatial autocorrelation [26]. In this regard, the indicator was Moran's I coefficient. The spatial linkages of the study units were specified using a weight matrix, which meant that units that were adjacent to one another in space were given more weight in the computation than those that were farther apart [27]. Pearson's correlation coefficient is extended to geographical neighbors by Moran's I. It provides a score in the range of -1 and 1. The null hypothesis—that there is no clustering—is represented by a score of zero. While a negative score suggests that nearby locations typically have differing attribute values, a positive score shows that places with comparable attribute values are clustered together [26]. Monte Carlo randomization was used to evaluate Moran's I significance. Statistical significance computation evaluates the Moran's I statistic's significance in relation to the null hypothesis [26, 29].

Hot spot analysis

The hot spot analysis (Getis-Ord Gi*) tool in ArcGIS 10.8 software was used to determine the Getis-Ord Gi* statistic for features. By comparing the local sum of the values for the feature in question and its neighbors to the sum of all feature values, the Getis-Ord Gi* statistic is computed [28]. Z-score was obtained from Gi*statistic for positive Z-scores; the larger Z-score reflects the more intensity of the clustering high values. For negative Z-scores, the smaller Z-score represents the more intense and the clustering of low values (i.e., a cold spot is obtained) [29].

Anselin local Moran's I analysis

Local Moran's in Anselin I was utilized to give information about high-risk and low-risk areas. High-high, low-low (showing a clustering pattern), low-high, high-low (indicating an outlier pattern), and not significant are the five categories into which this index separates polygons. High-high (HH) indicates high-risk clusters or hotspots by highlighting regions with high death rates combined with their environs. Low-low (LL) patches, on the other hand, show low-risk clusters of death or cold spots and areas with low mortality [29]. In ArcGIS 10.8, we produced spatial weights using polygon contiguity edges and corners weight.

Spatial Scan Statistic

Martin Kulldorff created the spatial scan statistic and put it into a software application called SaTScan. To determine the approximate locations of statistically significant geographical clusters of tuberculosis (TB) mortality and to look into their existence, SaTScan v10.1 was utilized [30]. Statistics analysis [31] were conducted for all age groups in order to identify clusters in the population's TB mortality. The Poisson probability model assumption, which states that the number of events in a region is Poisson distributed based on a known underlying population at risk, was used to identify spatial high clusters. To identify the TB death clusters in the research area, a purely spatial analysis was conducted, ignoring the time dimension of the cases. A circular window was imposed on the map by the spatial scan statistic, which allowed the circle to traverse over the region. As a result, the window had various sets of nearby TB mortality at various places. If the window contained the centroid of the TB mortality, then that TB mortality was included in the window. The TB mortality was included in the window if it included the centroid of the TB mortality. Every circle's radius was gradually expanded from 0 to its maximum. As a result, the window never included more than half of the whole population that was at risk. The most likely cluster was the one with the highest likelihood, which was maximized across all window sizes and positions. The Monte Carlo hypothesis testing technique was used to determine its relevance. 999 random Monte Carlo repetitions of the data set were created with the null hypothesis that there were no notable clusters, assuming that the relative risk (RR) of TB mortality was the same inside the window as it was outside, in order to determine the distribution of the test statistic. Each replica's test statistic was determined. Because the analysis at a reduced threshold could identify smaller and more defined areas, the maximum size of the spatial window in this study was established at 50% and 25% of the population [32, 33].

3. Results and Discussion

The Iraq annual mortality rates for TB are shown in Table 1. for all age gender categories, rates varied from 0 to 1.75 per 100,000, The geographic variation of country-level mortality rates for all age gender are shown in Fig. 1. The value of Moran's indices was positive (p-value < 0.05, z-score >1.96) in year of 2019 during the study period indicating clustered characteristic of the TB mortality rates. While it was randomly spatial in other years. Annual values of the Moran's I are presented in Table 2.

The Getis-Ord Gi* statistic for TB mortality rates identified eastern and middle Iraq as shown (Fig. 2). The analysis confirmed that the province of Baghdad, Babil, Karbala, Diwaniyah, Wasit and the province of Maysan had statistically significant higher rates of TB mortality rates than the rest of the country. Figure 3 shows the areas for TB mortality rates clustering identified by Anselin's Local Moran's I. The analysis identified Ninawa,Dahuk,Arbil and Tam'mim provinces in northern Iraq, as a low-low cluster and insignificant throughout the 5 years covered by the study. The province of Maysan, Karbala, Babil, Diwaniyah, Baghdad and Wasit were identified as a High- High cluster of TB mortality rates for 2018-2020 years, while the province of Tam'mim was category high- low outlier for 2022 year.

Based on the 50% maximum window size, the spatial scan statistic detected 1 statistically significant cluster located in Southeastern of Iraq (Table 3, Fig. 4(A, B)). The most likely cluster was found around Dha qar, Maysan, Basrah, Diwaniyah, Muthanna, Wasit, Babil, Najaf, and Karbala, where 23 cases were observed, whereas 13.49 were expected (LLR= 4.71, P < 0.05). Secondary clusters were found in Ninawa, Dahuk, Karbala, Arbil, Tam'mim, Salah ad din, Sulaymaniyah, Diyala, and Anbar (LLR= 0.88, P > 0.05); located in the Northeastern of country. The statistically significant most likely and secondary of TB mortality rates clusters were mainly distributed from center to Northeast in Iraq (Table 4, Fig. 4(C, D)); for 25% maximum window size. The statistically significant most likely was found around Diwaniyah**,** Babil**,** Wasit, Karbala, Dha qar, and Najaf where 15 cases were observed, whereas 7.65 were expected (LLR= 3.65, P < 0.05), with secondary clusters in Northeast, Ninawa, Dahuk, Karbala, Arbil, Tam'mim, Salah ad din, Sulaymaniyah, Diyala, and Anbar (LLR= 0.88, P > 0.05).

An overview of Iraq's most recent TB spatiotemporal epidemiological state is given in this report. The findings showed that TB rates were declining between 2018 and 2022. Even though Iran's TB prevalence is declining, screening, preventive, control, and therapeutic measures are still necessary, particularly in high-risk regions like eastern and middle Iraq. The lowering of tuberculosis in Iraq has been greatly aided by free treatment,

greater public knowledge, better hygiene, the opening of new TB research institutes, and easier and faster access to TB testing. Crucially, it was discovered that the decrease in TB was especially noteworthy. Since tuberculosis is contagious, prompt detection and treatment can lower its incidence because it can spread to other people.

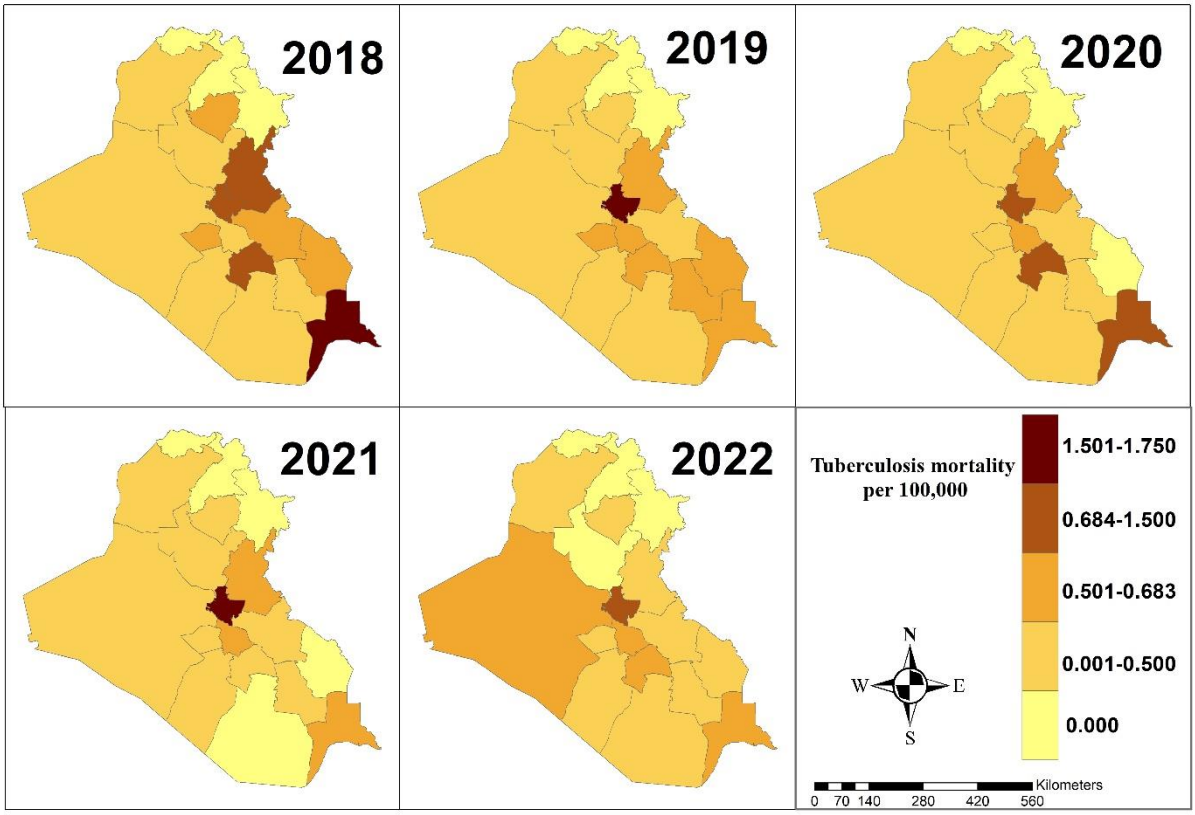

Fig. 1. Geographic distribution of TB mortality rates for all age gender in the Iraq, 2018–2022.

Table 1. Total annual mortality rates from TB in the Iraq, 2018 to 2022.

ID	Province	Annual 2018 Mortality Rate/100,000	Annual 2019 Mortality Rate/100,000	Annual 2020 Mortality Rate/100,000	Annual 2021 Mortality Rate/100,000	Annual 2022 Mortality Rate/100,000
1	Ninawa	0.255	0.305	0.229	0.382	0.305
2	Dahuk	0.000	0.000	0.000	0.000	0.000
3	Najaf	0.452	0.452	0.065	0.129	0.129
4	Karbala	0.545	0.857	0.234	0.390	0.156
5	Tam'mim	0.594	0.416	0.178	0.475	0.297
6	Baghdad	1.063	1.659	0.993	1.753	1.168
7	Muthanna	0.117	0.466	0.117	0.000	0.117
8	Babil	0.414	0.644	0.552	0.644	0.552
9	Diwaniyah	1.250	0.588	1.103	0.147	0.441
10	Dha qar	0.136	0.544	0.363	0.408	0.181
11	Basrah	1.600	0.686	0.979	0.849	0.555
12	Salah ad din	0.060	0.119	0.119	0.060	0.000
13	Anbar	0.268	0.322	0.429	0.322	0.429
14	Arbil	0.000	0.000	0.000	0.000	0.000
15	Diyala	1.160	0.638	0.638	0.754	0.174
16	Sulaymaniyah	0.000	0.000	0.000	0.000	0.000
17	Wasit	0.551	0.207	0.413	0.275	0.069
18	Maysan	0.683	0.512	0.000	0.000	0.085

Table 2. The global spatial autocorrelation for Moran's I from 2018 to 2022.

Year	Moran's I	Expected I	Variance	z-score	P-value	Pattern
2018	0.0043	-0.0588	0.0142	0.5288	0.5970	random
2019	0.1804	-0.0588	0.0112	2.2574	0.0240	clustered
2020	0.0485	-0.0588	0.0144	0.8952	0.3707	random
2021	0.0128	-0.0588	0.0106	0.6944	0.4874	random
2022	-0.0388	-0.0588	0.0110	0.1905	0.8489	random

Table 3. Clusters of TB mortality among Iraq Province from 2018 to 2022 for 50 % SaTScan.

Approximate Location	Radius(km)	Observed	Excepted	RR	LLR	P-value
A- Dha qar, Maysan, Basrah , Diwaniyah , Muthanna, Wasit, Babil, Najaf, and Karbala.	287.31	23	13.49	2.66	4.71	0.034
B- Ninawa , Dahuk , Karbala, Arbil, Tam'mim, Salah ad din ,Sulaymaniyah, Diyala ,and Anbar.	348.07	10	6.68	1.66	0.88	0.802

Table 4. Clusters of TB mortality among Iraq Province from 2018 to 2022 for 25 % SaTScan.

Approximate Location	Radius(km)	Observed	Excepted	RR	LLR	P-value
C- Diwaniyah **,** Babil **,** Wasit, Karbala, Dha qar, and Najaf.	144.26	15	7.65	2.54	3.65	0.042
D- Ninawa , Dahuk , Karbala, Arbil, Tam'mim, Salah ad din. ,Sulaymaniyah, Diyala ,and Anbar.	348.07	10	6.68	1.66	0.88	0.744

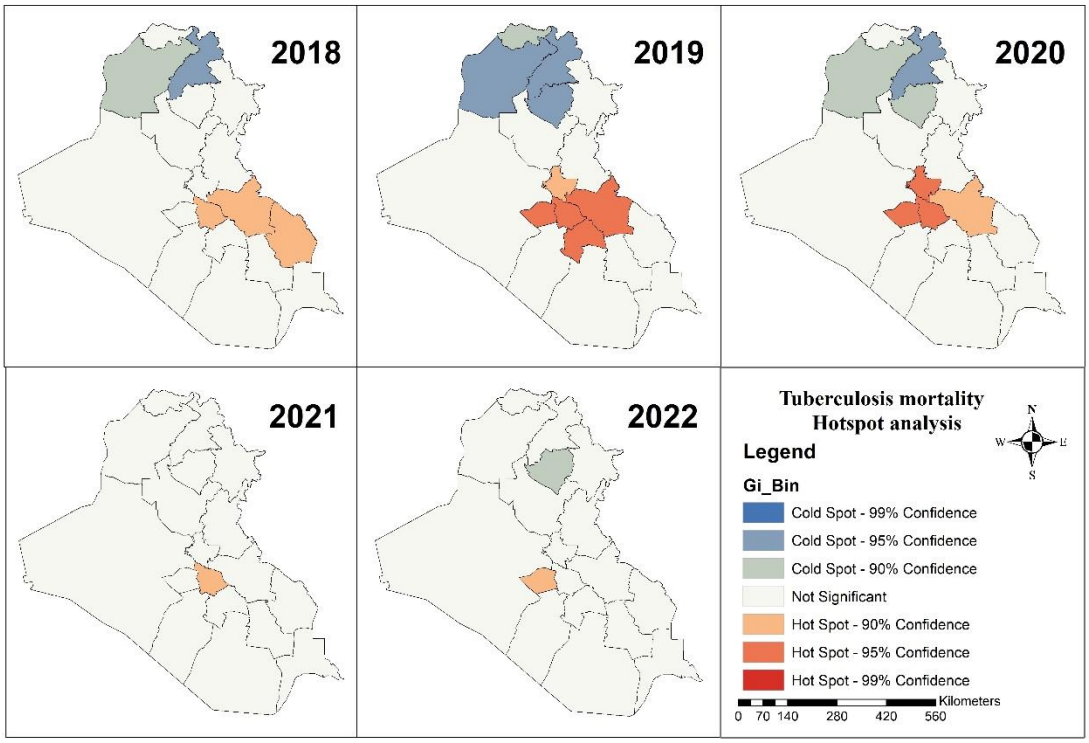

Fig. 2. Hot spot analysis of TB mortality rates for all age gender in the Iraq, 2018–2022.

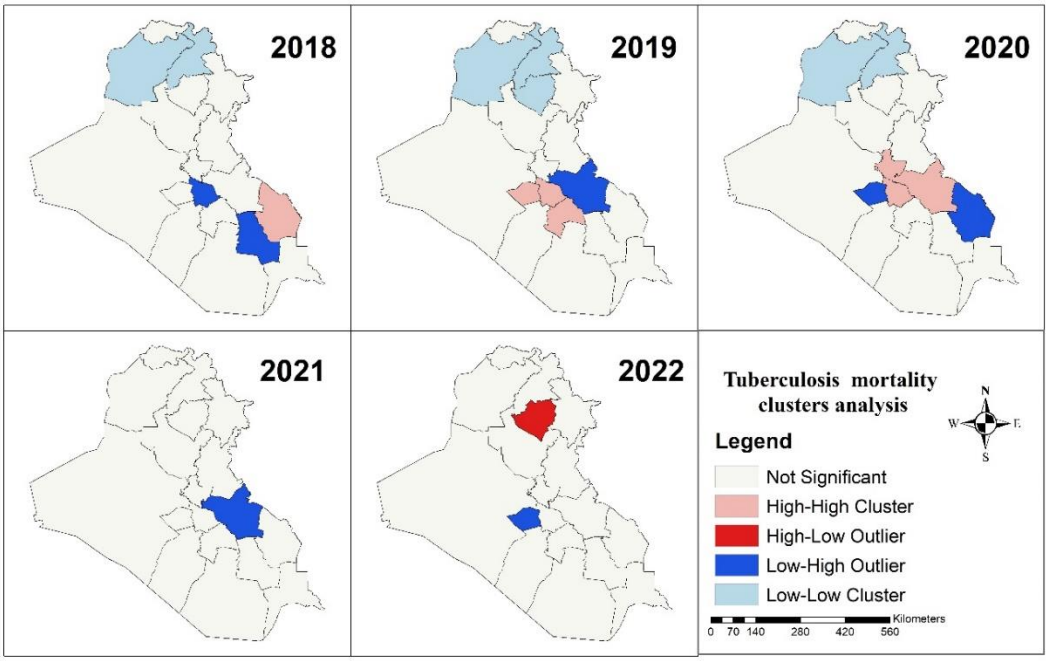

Fig. 3. Clustering analysis of TB mortality rates for all age gender in the Iraq, 2018–2022.

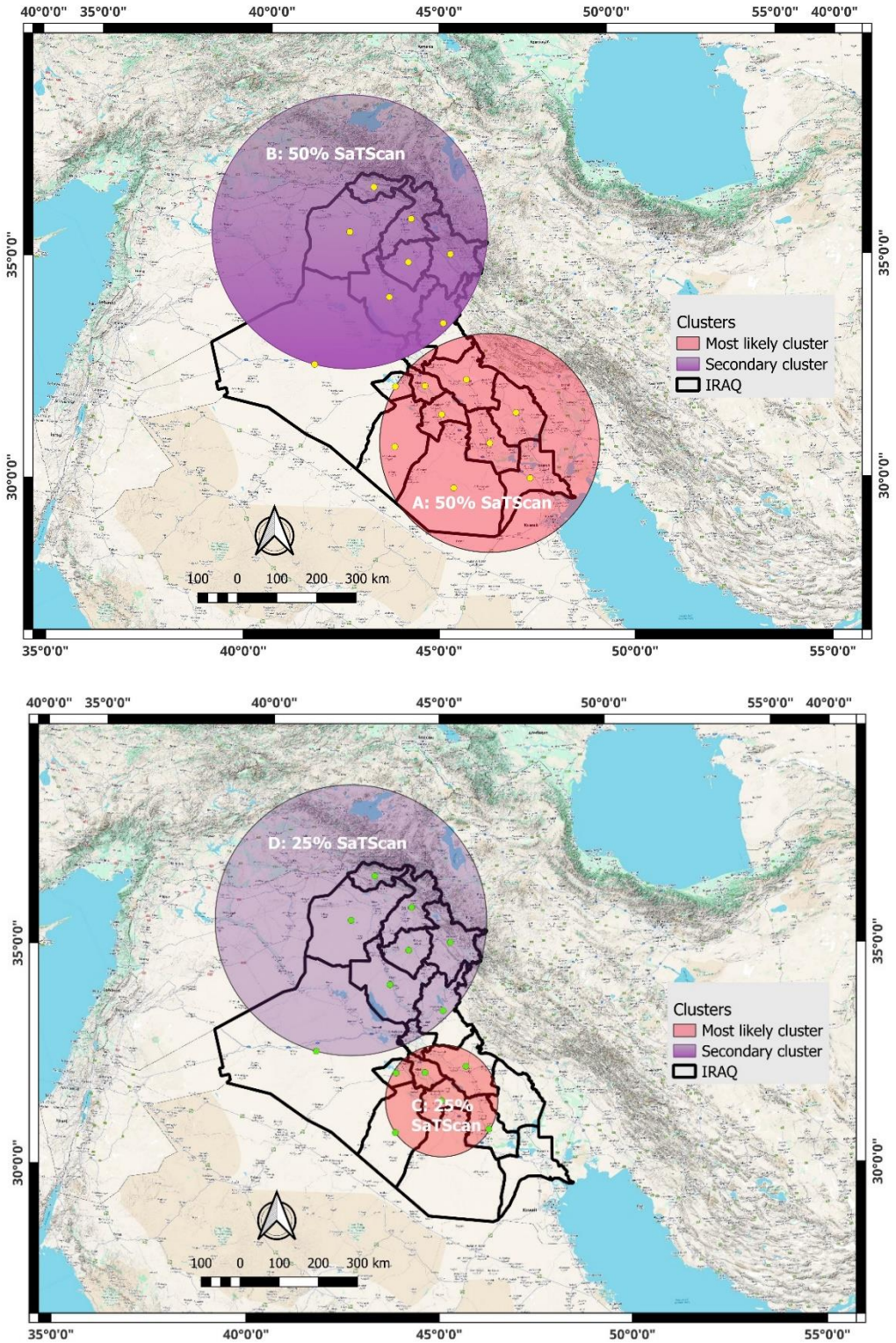

Fig. 4. Geographical clusters of TB mortality rates for all age gender (50% SaTScan-A, B, top) and (25% SaTScan-C, D, bottom) in the Iraq, 2018–2022.

References

1. World Health Organization. Global Tuberculosis Report 2021. https://doi.org/10.1016/j.ijid.2021.02.107
2. MacNeil A, Glaziou P, Sismanidis C, Maloney S, Floyd K. Global epidemiology of tuberculosis and progress toward achieving global targets—2017. Morb Mortal Wkly Rep. 2019;68(11):263–6. https://doi.org/10.15585/mmwr.mm6811a3.
3. Dirlikov E, Raviglione M, Scano F. Global tuberculosis control: toward the2015 targets and beyond. Ann Intern Med. 2015;163(1):52–8. https://doi. org/10.7326/M14-2210.
4. Dye C, Glaziou P, Floyd K, Raviglione M. Prospects for tuberculosis elimination. Annu Rev Public Health. 2013;34(1):271–86. https://doi.org/10.1146/annurev-publhealth-031912-114431.
5. Adin A, Lee D, Goicoa T, Ugarte MD. A two-stage approach to estimate spatial and spatio-temporal disease risks in the presence of local discontinuities and clusters. Stat Methods Med Res. 2019;28(9):2595–613. https://doi.org/10.1177/0962280218767975.
6. Local Burden of Disease HIVC. Mapping subnational HIV mortality in six Latin American countries with incomplete vital registration systems. BMC Med. 2021;19(1):4.
7. Goshayeshi L, Pourahmadi A, Ghayour-Mobarhan M, Hashtarkhani S, Karimian S, Dastjerdi RS, et al. Colorectal cancer risk factors in North-Eastern Iran: a retrospective cross-sectional study based on geographical information systems, spatial autocorrelation and regression analysis. Geospat Health. 2019;14(2):219–28.
8. Jaya IGNM, Folmer H. Bayesian spatiotemporal mapping of relative dengue disease risk in Bandung, Indonesia. J Geographical Syst. 2020;22(1):105–42. https://doi.org/10.1007/s10109-019-00311-4.
9. Shabanikiya H, Hashtarkhani S, Bergquist R, Bagheri N, VafaeiNejad R, Amiri- Gholanlou M, et al. Multiple-scale spatial analysis of paediatric, pedestrian road traffic injuries in a major city in north-eastern Iran 2015–2019. BMC Public Health. 2020;20:1–11.
10. Barman S, Sarkar A, Roy RK, Saha S, Rajak K, Sarkar J. An approach to GISbased traffic information system using spatial Oracle. Int J Spatial Temporal Multimedia Information Syst. 2019;1(3):253–71. https://doi.org/10.1504/ IJSTMIS.2019.103559.
11. Halimi L, Bagheri N, Hoseini B, Hashtarkhani S, Goshayeshi L, Kiani B. Spatialanalysis of colorectal Cancer incidence in Hamadan Province, Iran: a retrospective cross-sectional study. Appl Spatial Analysis Policy. 2020;13(2): 293–303. https://doi.org/10.1007/s12061-019-09303-9.
12. Hoseini B, Bagheri N, Kiani B, Azizi A, Tabesh H, Tara M. Access to dialysis services: a systematic mapping review based on geographical information systems. Geospat Health. 2018;13(1):3–10.
13. Kiani B, Bagheri N, Tara A, Hoseini B, Tabesh H, Tara M. Revealed access to haemodialysis facilities in northeastern Iran: factors that matter in rural and urban areas. Geospat Health. 2017. https://doi.org/10.4081/gh.2017.584.
14. Kiani B, Raouf Rahmati A, Bergquist R, Moghaddas E. Comparing spatiotemporal distribution of the most common human parasitic infections in Iran over two periods 2007 to 2012 and 2013 to 2018: a systematic quantitative literature review. Int J Health Plann Manag. 2020;35(5):1023–40. https://doi.org/10.1002/hpm.3010.
15. Jaya I, Andriyana Y, Tantular B, Ruchjana B. Spatiotemporal Dengue Disease Clustering by Means Local Spatiotemporal Moran's Index. IOP Conference Series: Materials Science and Engineering: IOP Publishing; 2019.
16. Ullah S, Daud H, Dass SC, Fanaee-T H, Kausarian H, Khalil A. Space-time clustering characteristics of tuberculosis in Khyber Pakhtunkhwa Province, Pakistan, 2015–2019. Int J Environ Res Public Health. 2020;17(4):1413. https://doi.org/10.3390/ijerph17041413.
17. Masabarakiza P, Hassaan MA. Spatial-temporal analysis of tuberculosis incidence in Burundi using GIS. J Public Health. 2019;5(6):280–6.
18. Sifuna P, Ouma C, Atieli H, Owuoth J, Onyango D, Andagalu B, et al. Spatial epidemiology of tuberculosis in the high-burden counties of Kisumu and Siaya, Western Kenya, 2012–2015. Int J Tuberculosis Lung Dis. 2019;23(3): 363–70. https://doi.org/10.5588/ijtld.18.0245.
19. Sharma, S.K., Mohan, A. and Kohli, M. Extrapulmonary tuberculosis. Expert Review of Respiratory Medicine, 2021. 15(7), pp.931-948. https://doi.org/10.1080/17476348.2021.1927718
20. Khabibullina, N.F., Kutuzova, D.M., Burmistrova, I.A. and Lyadova, I.V. The biological and clinical aspects of a latent tuberculosis infection. Tropical Medicine and Infectious Disease, 7(3), p.48.Tuberculosis Infection. Trop. Med. Infect. Dis., 2022. 7, 48. https://doi.org/10.3390/tropicalmed7030048
21. World Health Organization,. WHO consolidated guidelines on tuberculosis: module 2: screening: systematic screening for tuberculosis disease. 2021. World Health Organization. https://archive.lstmed.ac.uk/id/eprint/17349
22. World Health Organization. 2020. Global Tuberculosis Report. Incidence of Ttuberculosis (Per 100,000 People).

23. Ahmed, M. M. Tuberculosis Situation in Iraq: A puzzle of Estimates. In. J. Mycobacter, 2013. 2(4): 248-249. https://doi.org/10.1016/j.ijmyco.2013.10.002

24. Shoukrie, A., Alameen, A., Shaban, D., Alamari, M., Aboguttaia, N. and Askar, N. The Yield of Sputum Smear Direct Microscopy Using Ziehl-Neelsen Stain in Comparison with Lowenstein Jensen Culture on the Diagnosis of Pulmonary Tuberculosis in Tripo-li-Libya. Mycobact Dis, 2018. 8(1). DOI: 10.4172/2161-1068.1000256.

25. AL-Kaisse, A. A., AL-Thwani, A. N., Mankhi, A. A., Abood, Z. H., & Ali, R. M. (2023). Epidemiological study of prevalence TB in Iraq. Revis Bionatura, 8, 27.

26. Lai, P.C.; So, F.M.; Chan, K.W. Spatial Epidemiological Approaches in Disease Mapping and Analysis; CRC Press: New York, NY, USA, 2009.

27. *Moran, P.A.P. Notes on continuous stochastic phenomena. Biometrika 1950, 37, 17–23. [CrossRef] [PubMed]*

28. Kim S-M, Choi Y. Assessing statistically significant heavy-metal concentrations in abandoned mine areas via hot spot analysis of portable XRF data. Int J Environ Res Public Health. 2017;14(6):654.

29. *Peeters A, ZudeM, K¿thner J,-nlüM, Kanber R,Hetzroni A, et al. Getis–Ord's hot-and cold-spot statistics as a basis for multivariate spatial clustering of orchard tree data. Comput Electron Agric. 2015;111:140–50.*

30. Kulldorff, M. Software for the Spatial and Space-Time Scan Statistics. Available online: http://www.satscan.org (accessed on 24 September 2010).

31. Kulldorff, M. A spatial scan statistic. Commun. Stat. Theory Methods 1997, 26, 1481–1496. [CrossRef]

32. Tiwari, N.; Kandpal, V.; Tewan, A.; Rao, K.R.M.; Tolia, V. Investigation of tuberculosis clusters in Dehradun city of India. Asian Pac. J. Trop. Med. 2010, 3, 486–490. [CrossRef]

33. Agay-Shay, K.; Amitai, Y.; Peretz, C.; Linn, S.; Friger, M.; Peled, A. Exploratory spatial data analysis of congenital malformations (CM) in Israel, 2000–2006. ISPRS Int. J. Geoinf. 2013, 2, 237–255. [CrossRef]